POSITRON-PRODUCTION EXPERIMENT USING SILICON AND DIAMOND CRYSTALS IN THE KEKB 8-GEV INJECTOR LINAC

Tsuyoshi Suwada†, KEK, Tsukuba, Ibaraki, 305-0801 Japan.

Abstract

Intense positron sources are widely investigated for the next-generation of linear colliders and B-factories. A new method utilizing an axially-oriented crystal as a positron-production target is one of the bright schemes since it provides a powerful photon source through channeling and coherent bremsstrahlung processes when high-energy electrons penetrate the target. A series of positron-production experiments with heavy and light crystals hit by 4 and 8-GeV single-bunch electron beams have been carried out at the KEKB 8-GeV injector linac. This report gives the brief summary on the positron-production experiment using silicon and diamond crystals carried out in December 2002 at KEK. Later the report based on the more precise analysis will be published elsewhere.

1 INTRODUCTION

For future e^+e^- linear colliders and high-luminosity B-factories, it is critically important to develop a high-intensity positron source. In a conventional method using an amorphous heavy-metal target, the target thickness is optimized by taking into account the electromagnetic shower process and the positron capture efficiency in the succeeding acceleration section. The optimum thickness is 4-5 X_0 (radiation length) for a 4-8 GeV electron beam. In this case, the only possibility to increase the positron intensity is to increase the incident electron intensity. However, the electron intensity is limited due to a heat load on the target. One promising method utilizing a crystal target was proposed by Chehab *et al*. in 1994[1]. The benefit of this method is on its high positron-production efficiency due to channeling radiation (CR)[2] and coherent bremsstrahlung (CB), since CR and CB increase low-energy photons in the radiation process. This results in a thinner target compared with the conventional method. It is also expected that the thin target relaxes its heat load, and that the spatial spread of positrons due to multiple scattering in the target is reduced. Yoshida *et al*. demonstrated a clear enhancement of the positron yield in a tungsten crystal target using a 1.2-GeV electron beam[3]. This new scheme has been tested at the positron-production station and the end station of the KEKB injector linac[4]. Chehab *et al*. also studied the positron yield from a crystal target for 5-40 GeV electrons at CERN-SPS[5].

Although a positron enhancement is observed, there have so far been only a few experimental results over a wide energy range of a primary electron beam.

On the theoretical side, various simulation studies have been carried out by various authors. Among them, Baier, Katkov and Strakhovenko have developed the simulation code of the electromagnetic shower formation at axial alignment of a crystal by using the semi-phenomenological radiation spectrum[6]. This scheme allows one to consider a positron-yield enhancement at the relatively low energy range (a few GeV) of the initial electrons, which is suitable for the B-factory injector. The substantial enhancement of the positron yield from crystal targets is expected due to the increase in the number of relatively soft photons in comparison with that from an amorphous target. Thus, more systematic and precise experimental data could help us to understand the complicated mechanism of these elementary radiation processes and to design a high-intensity positron source. A series of experiments[7,8] to investigate the positron yields using various crystal targets are underway for an incident electron energy lower than 8 GeV. The following table shows a historical view of the positron-production experiments carried out at KEK-Tsukuba and KEK-Tanashi branch.

Table 1: Historical view of the positron-production experiments at KEK.

Month/Year	Accelerator	E [GeV]	Positron Target [mm]
May/1997	Tanashi/ES	1.2	Crystal W (W_c)[1.2]
Apr, Jun /1998	KEK/Linac	3	W_c[1.7] + Amor. W (W_a)[7]
Nov/1998	Tanashi/ES	0.6, 0.8, 1	W_c[0.4, 1.2, 2.2], GaAs[0.36], Diamond[1.1]
Sep, Oct /2000	KEK/Linac	8	W_c[2.2], W_c[2.2]+W_a[5,10,15]
Apr/2001	KEK/Linac	8	W_c[2.2], W_c[9] W_c[9]+W_a[2, 4]
Sep/2001	KEK/Linac	8	W_c[2.2], W_c[5.3], W_c[9] Combined targets
Jan/2002	KEK/Linac	4	W_c[2.2], W_c[5.3], W_c[9] Combined targets
Aug-Sep /2002	KEK/Linac	8	Si [2.6, 30, 48] Diamond[4.57] Combined targets
Dec/2002	KEK/Linac	8	Si [10, 30, 48] Diamond[4.57] Combined targets

†E-mail address: tsuyoshi.suwada@kek.jp.

2 EXPERIMENTAL SETUP

2.1 Beam Line

Our experiment was performed in the beam switchyard of the KEKB 8-GeV injector linac (see Fig.1).

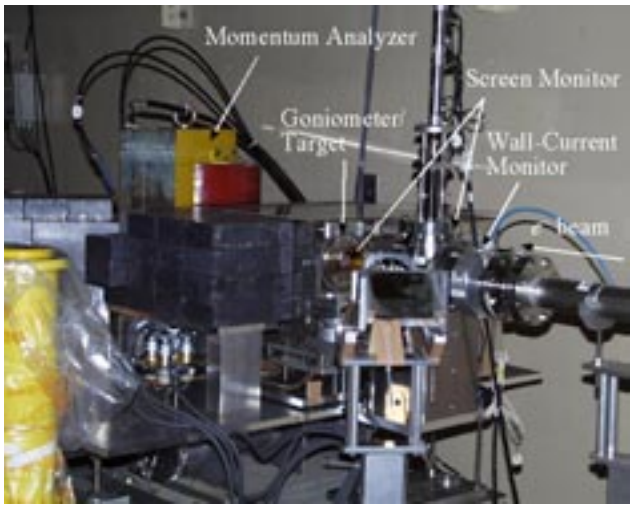

Figure 1: Photograph of the beam line and the experimental setup viewed from the electron beam.

An electron beam with a pulse width of 10 ps (S-band single bunch) and with an energy of 8 GeV impinged on a tungsten target at a repetition rate of 25 Hz. The beam charge (~0.1 nC/bunch) was measured by a wall-current monitor for each pulse. The transverse profile of the electron beam at the target was monitored by a screen monitor during the experiment. The transverse beam size was 0.8 mm (FWHM) in diameter. The angular spreads of the electron beam were expected to be about 22 and 44 μrad in the horizontal (*H*) and vertical (*V*) directions for the 8-GeV electrons, respectively. However, since the electron beam impinged on the target after passing through a vacuum window made of 30μm-thick stainless steel (SUS304), the angular spreads (*H* and *V*) of the electron beam at the target were estimated to be 59 and 70 μrad in total by taking into account the multiple scattering at 8 GeV, respectively. The multiple scattering effect of the vacuum window was investigated by using SUS foils with several thicknesses. These angular spreads were less than the critical angles (170 μrad for Si crystal and 130 μrad for Diamond crystal) of the channeling condition at 8 GeV.

2.2 Experimental Setup

Figure 2 shows a schematic drawing of the experimental setup. This comprises a positron-production target mounted on a precise goniometer, a magnetic spectrometer, collimators, and two kinds of positron detectors (a lead-glass calorimeter and an acrylic Cherenkov counter). All of the collimators and detectors are installed in a vacuum chamber kept at a vacuum pressure of 10^{-1} Pa.

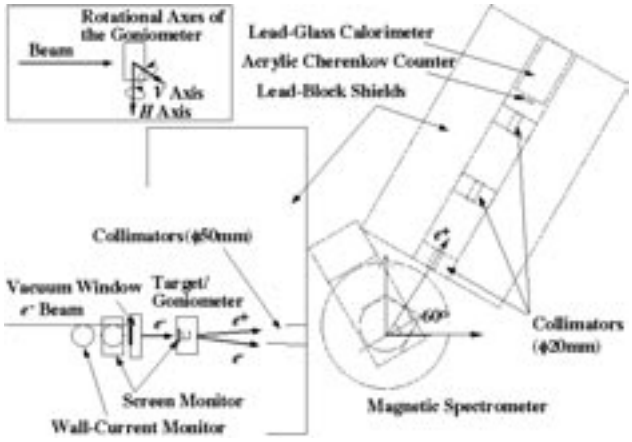

Figure 2: Schematic drawing of the experimental setup.

In this experiment, silicon and diamond crystals of <110> axis with different thicknesses were tested either alone or in combination with an amorphous tungsten plate (W_a). These W_as' with different thicknesses from 3 to 18 mm by 3mm steps are installed on a horizontal movable stage 82.5 mm after the crystal target. These tungsten plates were also used to calibrate the positron yield without the crystal targets. The specification of the crystal targets is summarized in Table 2.

Table 2: Tested crystal specification.

Crystal	Elem.	Denom.	Thickness [mm]	X_0
Diamond	C	5mmDia	4.57	0.0372
Silicon	Si	2.5mmSi	2.55	0.0272
Silicon	Si	10mmSi	9.9	0.1058
Silicon	Si	30mmSi	29.9	0.319
Silicon	Si	50mmSi	48.15	0.514

*$1X_0$=123mm (Diamond), $1X_0$=93.6mm (Silicon). It should be noted that the radiation length of an amorphous carbon (2.3 g/cm^3) is different from that of a diamond crystal (3.5 g/cm^3). This was pointed out by A. Potylitsyn.

The positrons emitted from the target in the forward direction were momentum-analyzed in a momentum range lower than 30 MeV/c by the magnetic field, where the deflection angle was 60^o from the beam axis. The positron trajectory was determined by five collimators installed before and behind the magnetic spectrometer. The geometrical acceptance and momentum acceptance is summarized in Table 3, which were calculated by using the simulation code GEANT3.

The momentum-analyzed positrons were detected with a 3mm-thick acrylic Cherenkov counter and a lead-glass calorimeter shielded by lead blocks. The lead blocks suppressed any background caused by electromagnetic showers generated upstream of the beam line due to the

off-momentum electrons, and caused by electromagnetic showers generated at the collimators. Since the emitted positrons were also shortly bunched, the number of positrons per bunch was measured as a pulse charge from each detector. Signals from the positron detectors and the signal of the electron beam charge were sent to a data-acquisition system using a PC-based CAMAC/ADC system, where all signal charges were simultaneously digitized. The goniometer could rotate the crystal target around two axes (*H* and *V* axes) by a pulse motor. The angular resolutions of the goniometer were 10.5 and 34.9 μrad/pulse in the *H* and *V* axes, respectively. The crystal axis, <110>, was determined by changing the relative rotational angles around the two axes with a step of 2 (or 1) mrad. The positron yields were measured for each target as a function of the rotational angle of the goniometer and as a function of the positron momentum.

Table 3: Acceptance of the positron spectrometer.

Pe^+ (MeV/c)	Acceptance (10^{-4} x (MeV/c•sr))
5	1.08 ± 0.03
10	2.47 ± 0.07
15	3.80 ± 0.10
20	4.81 ± 0.12

3 EXPERIMENTAL RESULTS

3.1 Two-Dimensional Crystal Axis Scan

We developed a computer software which quickly scans a crystal axis in two dimensional plane. The scanning time (10~20 min depending on the step sizes) was much reduced compared with that of the previous one-dimensional scanning. Figures 3(a) and 3(b) show the typical results of the crystal axis scanning measured for the diamond and 30mm-thick silicon crystal, respectively, at the positron momentum of 20 MeV/c.

You can clearly see main sharp peaks for both the crystals generated from the <110> axis orientation together with many weak peaks. The main sharp peak was formed as the intersecting point of the several lines (see the density distribution in the projected plane in Fig.3). These weak peaks or lines may come from plane channeling in the crystal. It is interesting that the number of the weak peaks for the diamond crystal is larger than that of the silicon crystal.

3.2 Rocking Curves

Figures 4(a) (for diamond) and 4(b) (for 30mm-thick silicon) show the measured rocking curves at the positron momentum of 20 MeV/c. You can see very narrow peak widths for both the crystals. The peak widths were obtained to be 0.7 (for diamond) and 1 mrad (for 30mm-thick silicon) in one sigma by the least-squares fitting procedures with two gaussian functions.

Figure 5 shows the variation of the peak width as a function of the crystal thickness in unit of X_0. The peak width increases gradually with the increase of the crystal thickness and its value is about 1 mrad level depending on the crystal thickness.

3.3 Positron-Yield Enhancement

Figure 6 shows the result of the positron-yield enhancement measurement for the crystal alone as a function of the crystal thickness in unit of X_0 at the positron momentum of 20 MeV/c. The enhancement of the silicon crystal changes by a factor of 8-14 depending on the crystal thickness, and for the diamond it is about 17 which is clearly larger than that of the silicon crystals. It means that the crystal effect of the diamond is larger than that of the silicon.

Figure 7 shows the result of the momentum dependence of the positron-production enhancement. The enhancement is slightly dependent on the positron momentum in the measured region.

Figure 8 shows the summarized result of the enhancement measurement together with the tungsten crystal data, which were obtained from the previous experiment. The result shows that although in the region of the thin thickness the enhancement obtained for the light crystals is a little bit high, in the region of the large thickness the enhancement obtained for the tungsten crystals is clearly higher. It is presumed that the channeling photons generated from the light crystal are soft, and thus, the positrons generated in the later amorphous tungsten are absorbed and multiply scattered in the target because they are also soft.

3.4 Positron Yields and Crystal Effect

The detected positron yields were calibrated by using the data from the amorphous tungsten plates with different thicknesses. Figure 9 (a) shows the variations of the positron yield depending on the thickness of the amorphous tungsten plates alone, and they were obtained as the positron-yield calibration data in each crystal measurement. For all the amorphous tungsten data, the positron yield was normalized by using the data of the 9mm-thick amorphous tungsten obtained in the 30mm-thick silicon crystal measurement. Figure 9 (b) shows the variations of the positron yield depending on the total thickness in unit of X_0, where the crystal axis was set in the direction of off axis. These results show that the positron-yield normalization was performed quite well within the experimental accuracy.

Figure 10 shows the summarized result of the normalized positron yield obtained for all the crystal measurements. It is clearly found several following things:

- The maximum positron yield is almost the same level compared with that of the amorphous tungsten except for the data of the 10mm-thick silicon crystal.
- The shower maximum thickness of each crystal is reduced compared with that of the amorphous

tungsten, which means that the radiation thickness is effectively reduced.

- The reduction of the shower maximum thickness of the diamond crystal is relatively large compared with other crystals although the thickness of the diamond is thin.

Figure 11 shows the result of the crystal effect. If we plot the shower maximum peak thickness as a function of the crystal thickness, we can estimate how large the crystal effect is. For the silicon crystal, the effect is saturated around the thickness of 30 mm, and for the diamond crystal, although we have only one data point, the effect is larger than the silicon crystal. This result shows that the maximum positron yield from the 5mm-thick diamond crystal is almost the same level as that of the 30mm-thick silicon crystal, which gives larger crystal effect than that of the diamond even with a 5mm-thcikness. We can expect higher positron-production yield if we use a thicker diamond crystal.

3.5 Effect of the Vacuum Window

Figure 12 shows the result of the positron enhancement measurement depending on the thickness of the vacuum window, where the diamond crystal alone was used in this test. From the result, the enhancement is almost constant up to the window thickness of 200 μm, and the rocking-curve peak width slightly increases with the increase of the window thickness. This may come from the increase of background generated at the window. It is noted that the window thickness of 100 μm has been used in the previous channeling experiment.

4 SUMMARY

The positron-production experiment using diamond and silicon crystal targets has been successfully carried out at the KEKB 8-GeV injector linac. The obtained rocking peak widths are very narrow less than 1 mrad in one sigma for both the crystals. For the crystal target alone, the enhancements of the positron yield are 9.3±0.5 (10mmSi), 9.9±0.5 (30mmSi), 6.4±0.3 (50mmSi), and 16±0.8 (5mmDiamond) at the positron momentum of 20 MeV/c. The enhancement is much reduced with the increase of the total target thickness. The maximum positron yields are the same level as the maximum yield obtained for amorphous tungsten targets.

5 REFERENCES

[1] R.Chehab, Orsay Report No. LAL/RT94-09, 1994.
[2] A.H.Sorensen and E.Uggerhoj, Scientific American June (1989) 70.
[3] K.Yoshida, *et al.*, Phys. Rev. Lett. 80, 1437 (1998).
[4] I. Abe, *et al.*,"The KEKB Injector Linac"; KEK-Preprint-2001-157 (2001); To be published in NIM A.
[5] R. Chehab, *et al.*, RREPS01, Lake Aya, Russia, September 2001, published in NIM **B103** (2003) 243.
[6] V.N. Baier, V.N. Katkov and V.M. Strakhovenko, NIM **B103** (1995) 147.
[7] H. Okuno, *et al.*, RREPS01, Lake Aya, Russia, September 2001, published in NIM **B103** (2003) 259.
[8] T.Suwada, *et al.*, Phys. Rev. **E67**, 016502 (2003).

(a)

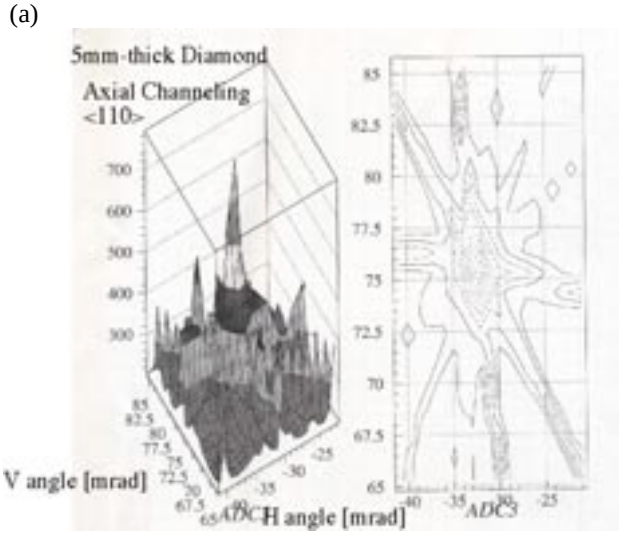

(b)

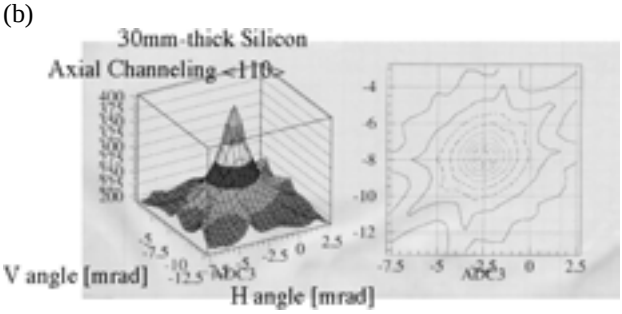

Figure 3: Results of the two-dimensional axis scan for (a) the diamond and (b) silicon crystal. The software of the axis scan was developed by Tokyo Metropolitan Univ.

(a)

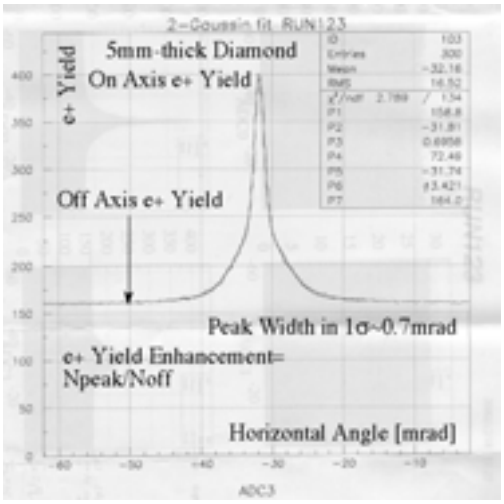

(b)

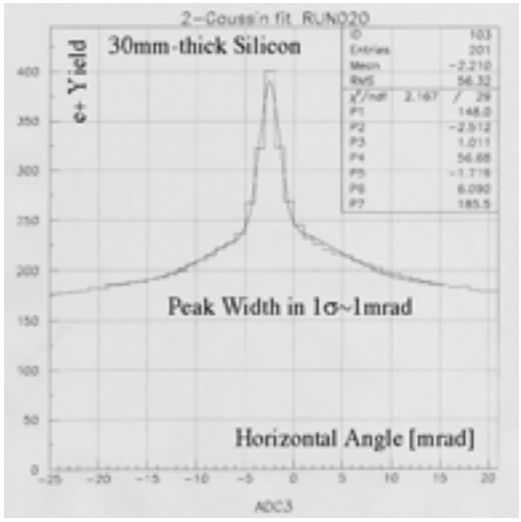

Figure 4: Rocking curves measured for (a) the 5mm-thick diamond and (b) 30mm-thick silicon crystal at the positron momentum of 20 MeV/c.

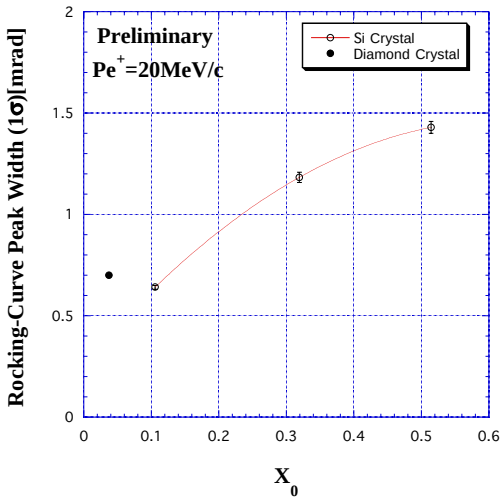

Figure 5: Variations of the rocking-curve peak width measured for (a) the diamond and (b) silicon crystal as a function of the crystal thickness at the positron momentum of 20 MeV/c.

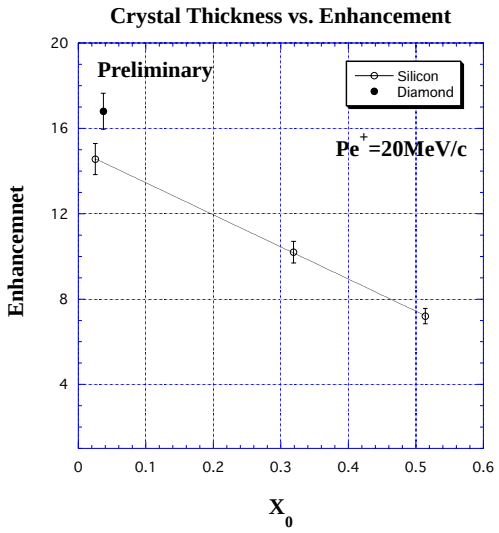

Figure 6: Variations of the positron yield enhancement depending on the crystal alone thickness in unit of X_0 at the positron momentum of 20 MeV/c.

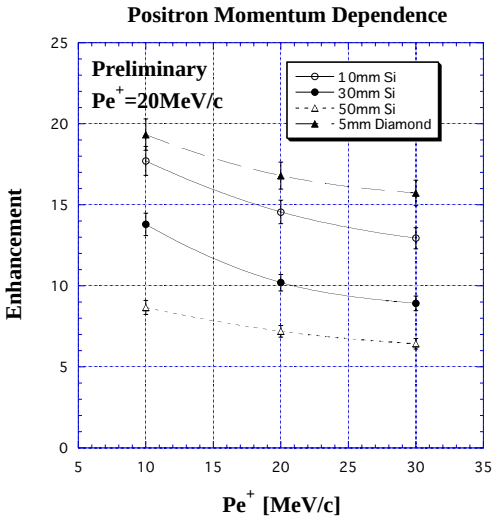

Figure 7: Variations of the enhancement depending on the positron momentum.

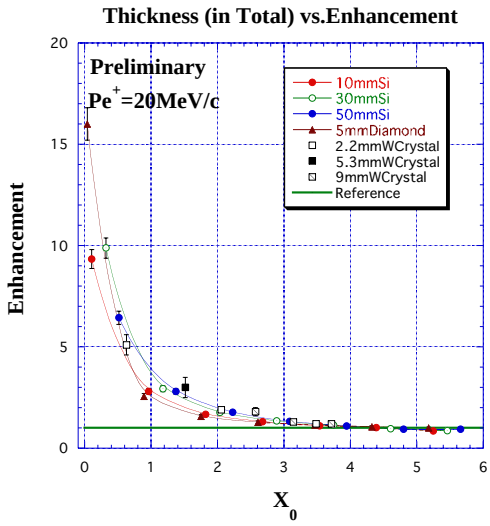

Figure 8: Variations of the positron-yield enhancement depending on the target thickness in total in unit of X_0 at the positron momentum of 20 MeV/c. The crystal tungsten data with three different thicknesses are also added.

(a)

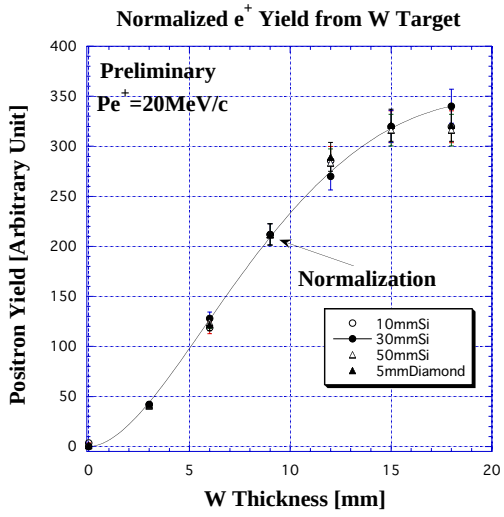

(b)

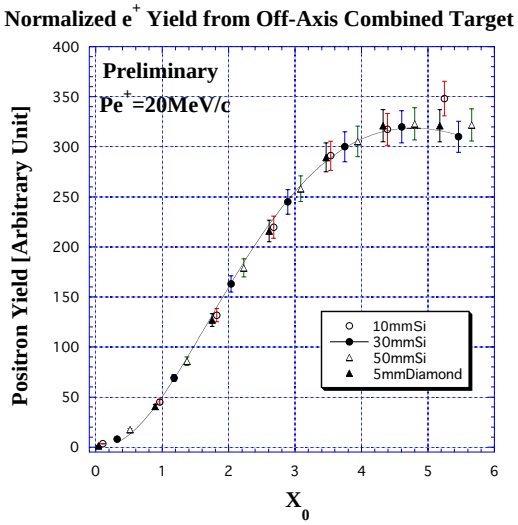

Figure 9: Variations of the shower development curve (positron yield) for (a) the amorphous tungsten plate alone and (b) off-axis combined target depending on the thickness of the combined target at the positron momentum of 20 MeV/c.

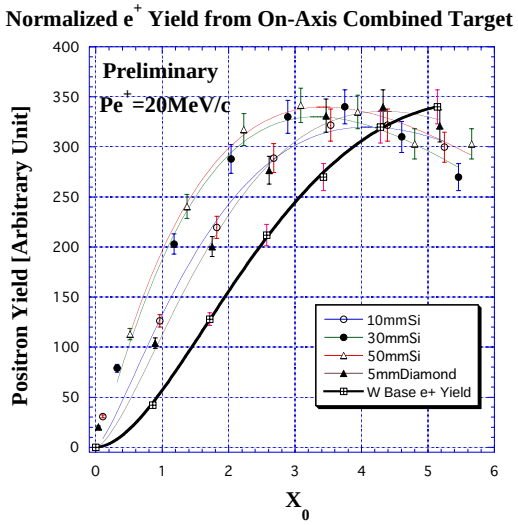

Figure 10: Shower development curves (positron yields) measured for the diamond and silicon crystal as a function of the combined target thickness in total at the positron momentum of 20 MeV/c.

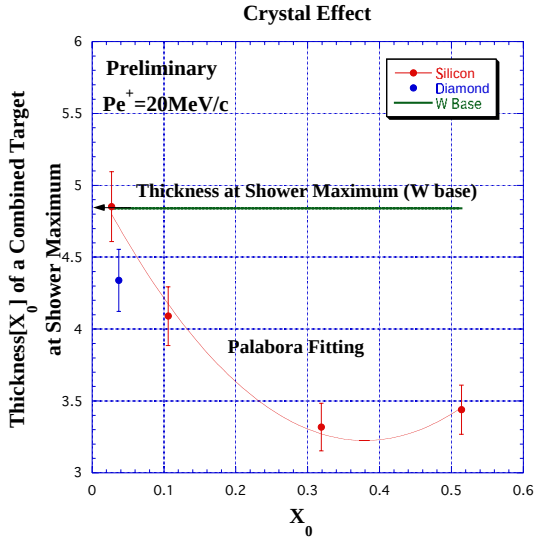

Figure 11: Variations of the crystal effect for the diamond and silicon crystal depending on the crystal thickness.

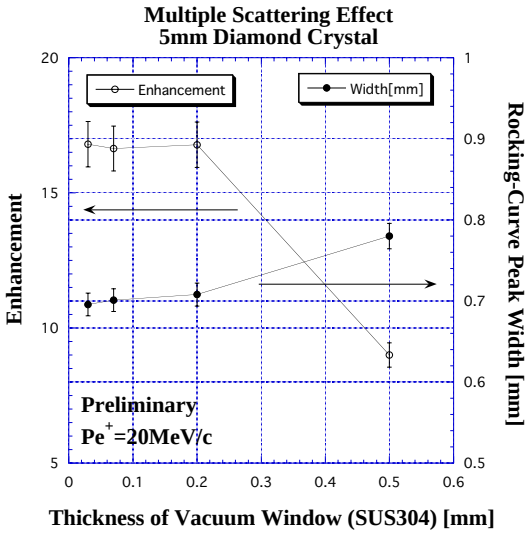

Figure 12: Vacuum-window thickness effect. The effect was estimated by using two parameters “Enhancement” and “Peak width” of the diamond crystal data as a function of the thickness of the vacuum window.